

Advanced Materials and Application III

Selected peer-reviewed full text papers from
3rd International Symposium on
Advanced Materials and Application
(ISAMA 2020)

Edited by
Mosbeh Kaloop

TTP TRANS TECH PUBLICATIONS

Preface

The 2020 International Symposium on Advanced Materials and Application (ISAMA 2020) was taken place in Seoul, South Korea, on February 14-16, 2020.

The objective of ISAMA 2020 is to bring together academics, scientists, engineers, postgraduates, and other professionals in the area of materials science and engineering technology from all over the world. It provides a high-standard international forum to introduce, to exchange, and to discuss recent advances novel and practical techniques or application in the field of materials engineering.

We would like to thank the program chairs, organization staff, and the members of the program committee for their work. Thanks also go to all those who have contributed to the success of ISAMA 2020. We hope that all participants and other interested readers benefit scientifically from the proceedings and also find it stimulating in the process.

The Organizing Committee of ISAMA 2020

Committee Chair

Prof. Mosbeh Kaloop Incheon National University
Incheon Disaster Prevention Research Center

Committees

Organizer

Prof. Mosbeh Kaloop Incheon National University
Incheon Disaster Prevention Research Center

Secretary

Heysu Ji ISAMA Committee

Associate Editors

Prof. Mosbeh Kaloop Incheon National University
Prof. Jungkyu Ahn Incheon National University

Technical Committee

Prof. Dongkeon Kim Dong-A University

Table of Contents

Preface

Drying Characteristics of <i>Chlorella pyrenoidosa</i> Using Oven and its Evaluation for Bio-Ethanol Production	
Megawati, A. Damayanti, R.D.A. Putri, I.N. Pradnya, H.F. Yahya and N.K. Arnan	1
Reduction of Surface Cracks at Al-Mg Alloy Strip Surface Cast by Unequal Diameter Twin Roll Caster	
T. Haga, K. Yamazaki, H. Watari and S. Nishida	6
Roll Casting and Die Casting of Si-Added Al-Mg Alloy	
T. Haga, S. Imamura, H. Fuse, H. Watari and S. Nishida	12
Effect of Si and Mn Addition on Fluidity, Mechanical Property and Casting Crack in Die Casting	
H. Fuse, S. Imamura and T. Haga	18
Casting of Clad Strip Consisting of Al-Sn Alloy and Pure Aluminum	
T. Haga	23
Changing from a Vertical Burr to a Horizontal Burr in the Vertical-Type High-Speed Twin-Roll Caster	
T. Haga, Y. Murakami, S. Kitamura, H. Watari and S. Nishida	29
Globular Crystals in the Center of Roll Cast Aluminum Alloy Strips	
T. Haga, M. Tsuchida, H. Sakata, H. Watari and S. Nishida	34
Effect of Alloying Elements on Mechanical Properties of High-Strength Low-Alloy Steel	
N. Li, W. Kingkam, Z.M. Bao, R.H. Han, Y. Huang, H.X. Zhang and C.Z. Zhao	41
Effect of Synthesis Conditions on the Preparation of Ag/ZnTiO₃ via Sol-Gel Method and its Antibacterial Properties	
H.T.A. Le, T.A. Nguyen and K.P.H. Huynh	47
Pebax 1657 Nanocomposite Membranes Incorporated with Nanoadsorbent Derived from Oil Palm Frond for CO₂/CH₄ Separation	
A.A. Ghazali, S.A. Rahman and R.A. Abu Samah	52
Mechanochemical Synthesis of Zinc Oxide Nanoparticles and their Antibacterial Activity against Escherichia Coli	
T.A. Nguyen, T.Y. Mai, T.X.M. Nguyen, K.P.H. Huynh, M.V. Le and T.A.N. Nguyen	59
Geopolymer Synthesis Using Metakaolin and High Calcium Fly Ash as Binary System Geopolymer	
T. Pantongsuk, C. Tippayasam, P. Kittisayarm, S. Nilpairach and D. Chaysuwan	65
Synthesis of Magnetically Separable Activated Carbon from Pineapple Crown Leaf for Zinc Ion Removal	
W. Astuti, T. Sulistyaningsih, D. Prastiyanto, B.S.A. Purba and R. Kusumawardani	71
An Innovative Method of Voided Reinforced Concrete One-Way Slabs Using Bundled Waste PET Bottled Tubes	
M.S. Mohammed, M.L. Ahmed, Z.M. Ali and A.S. Mahmoud	76
The Effect of Volumetric Hydrophobization on Moisture Transfer during Hardening of Concrete	
S.V. Fedosov, V.E. Roumyantseva and V.S. Konovalova	85
Rice Husk Ash as a Cement Replacement in High Strength Sustainable Concrete	
A. Ahmed, F. Hyndman, J. Kamau and H. Fitriani	90
Effect of Temperature on Phase Angle and Dynamic Modulus of Asphalt Mixtures Using SPT	
J. Ahmad, M.R. Hainin, E. Shaffie, K.A. Masri and M.A. Shaffi	99
Non-Destructive Detection of GIS Aluminum Alloy Shell Weld Based on Oblique Incidence Full Focus Method	
X.X. Wang, C. He, P.Z. Zhao, Y. Zheng, S.H. Jiang and Y.D. Wei	105
Mechanical Characterization of a Masonry System Made of Alkaline Activated Pozzolana Blocks	
J. Salirrosas, G. Silva, S. Kim, J. Nakamatsu, B. Bertolotti and R. Aguilar	111

A Study of Thermal Conductivity Property of Socks W.Y. Wang, K.T. Hui, C.W. Kan, K. Viseshpan, S. Areechongchareon, S. Tiyasri and R. Mongkholrattanasit	118
Evaluating the Air Permeability Properties of Summer Cooling Towels Y.L. Lam, W.Y. Wang, C.W. Kan, K. Manarungwit, W. Changmuong, J. Pattavanitch, W. Wongphakdee and R. Mongkholrattanasit	125
Bioactive Membranes of Polymeric Micro and Nanocomposites Prepared with the Natural Anionic Marine Polysaccharide (Alginate) Functionalized with Extracts of Cat's Claw (<i>Uncaria tomentosa</i>) and <i>Aloe vera</i> S. Kim, M. Elgegren, A. Donayre, B. Galaretta and J. Nakamatsu	131
Oxidation Behavior of TiC/Mo Composites by Spark Plasma Sintering Y.L. Liu, Y.Q. Zhu, X.K. Yang, Z.M. Bao, R.H. Han, H.X. Zhang and C.Z. Zhao	137
Synthesis Study of Silver-Doped Zinc Oxide for Near-Infrared Shielding Applications S. Kaenphakdee, S. Yodyingyong, J. Leelawattanachai, W. Triampo, N. Sanpo, J. Jitputti and D. Triampo	143
Effect of Morphology on Near-Infrared Shielding Properties of Aluminum-Doped ZnO by Solvothermal Synthesis P. Putthithanas, S. Yodyingyong, J. Leelawattanachai, W. Triampo, N. Sanpo, J. Jitputti and D. Triampo	148
Characterization of Semi-Refined Carrageenan Reinforced with Cellulose Nanofiber Incorporated α-Tocopherol for Active Food Packaging Applications W.A. Wan Yahaya, R.N. Raja Ahmad and N.A. Mohd Azman	154
Analysis of Pitting Corrosion for 2219 Aluminium Alloy under Different Corrosion Circumstances Y.F. Li and S.L. Lv	160
Reviews on Different Types of Rooftile BIPV: Materials Point of View N. Safitri, R. Syahyadi, F. Rizal and Y. Yassir	165

Synthesis of Magnetically Separable Activated Carbon from Pineapple Crown Leaf for Zinc Ion Removal

Widi Astuti^{1,a*}, Triastuti Sulistyaningsih^{2,b}, Dhidik Prastiyanto^{3,c}, Bernadetta Sisca Aprillia Purba^{1,d} and Restu Kusumawardani^{1,e}

¹Chemical Engineering Department, Universitas Negeri Semarang, Semarang 50229, Indonesia

²Chemistry Department, Universitas Negeri Semarang, Semarang 50229, Indonesia

³Electrical Engineering Department, Universitas Negeri Semarang, Semarang 50229, Indonesia

^awidi_astuti@mail.unnes.ac.id, ^btriastuti.s@mail.unnes.ac.id,

^cdhidik.Prastiyanto@unnes.ac.id, ^dbernadettasap@gmail.com, ^erestuk41@gmail.com

Keywords: Activated carbon, Adsorption, Magnetite, Metal removal, Pineapple crown leaf

Abstract. Metals removal from wastewater has become a major concern over the years due to the adverse effects of metals on organisms and environment. Adsorption is one of the safest, simplest, and most cost-effective methods for metals removal. The primary purpose of this study was to develop a magnetically separable activated carbon from pineapple crown leaf for zinc removal. Magnetic activated carbon (MAC) were characterized by SEM-EDX and FTIR. The ability of MAC to adsorb zinc ion was studied through variation of initial solution pH, concentration, and contact time. The optimum pH for zinc removal was four, while the equilibrium was reached after 180 min. In this condition, the percentage removal of zinc was 70.5%.

Introduction

Wastewater discharged by industries is one of the heavy metal pollution sources. The hazardous compounds contained in the wastewater (e.g., zinc ion (Zn^{2+})) cause a serious environmental pollution problem if the concentration exceeds the water quality standard. Zn^{2+} can accumulate in organism tissue, causing numerous diseases such as anemia, kidney damage, stomach cramps, and nausea [1]. Several methods have been developed for heavy metals removal from wastewater such as ion-exchange [2], chemical precipitation [3], membrane filtration [4], electrochemical [5], coagulation [6], and adsorption [7]. Among them, adsorption is one of the safest, simplest, and most cost-effective methods for metals removal [1]. In this sense, activated carbon (AC) produced from biomass waste such as pineapple crown leaf [7, 8] is considered an efficient adsorbent due to it has a high adsorption capacity and abundant availability. Pineapple crown leaf (*Ananas comosus*) is composed of 70-80% α cellulose, 5-12% lignin, and hemicellulose, which enable it to act as a precursor in the synthesis of AC [8]. However, operating conditions during AC preparation affect the characteristics and performance of the obtained AC.

Modification of AC using chemical treatment including KOH [9], $ZnCl_2$ [9], H_3PO_4 [10, 11], or K_2CO_3 [12] has been studied. In this sense, conventional heating using an electric furnace was usually adopted [13]. Although AC has been widely used for metal removal in wastewater, the separation of AC from solution is still an important matter. Sedimentation, filtration, and centrifugation, which are usually used after the adsorption process are considered uneconomic and time-consuming [14]. The use of magnetic activated carbon (MAC) becomes a viable alternative to solve the problem. However, the loading of magnetite (Fe_3O_4) in AC requires a detailed investigation to increase its adsorption capacity. Therefore, the aims of this work were to (1) prepare MAC from pineapple crown leaf waste with KOH activation, and (2) investigate zinc (Zn^{2+}) adsorption characteristics by MAC.

Materials and Methods

Materials. Ferrous sulfate hydrate ($\text{FeSO}_4 \cdot 7\text{H}_2\text{O}$), ferric chloride hexahydrate ($\text{FeCl}_3 \cdot 6\text{H}_2\text{O}$), zinc nitrate tetrahydrate ($\text{Zn}(\text{NO}_3)_2 \cdot 4\text{H}_2\text{O}$), potassium hydroxide (KOH) pellets, sodium hydroxide (NaOH), and hydrochloric acid (HCl) were supplied by Merck (Germany).

Activated Carbon (AC) Preparation. Pineapple crown leaf was chopped, washed, dried at 110°C in an electric oven (Memmert type UN55, Germany) for 24 hours, and blended to a powder. The powder was then carbonized in an electric furnace (Model FB1310M-33 Thermolyne, Thermo Scientific, USA) at 500°C for 90 min in limited air [8]. The resulting char was then impregnated with 8.75 g KOH and 10 mL of distilled water for 120 min. The impregnation ratio of 1.75: 1 g/g of KOH to char. Furthermore, the sample was dried at 105°C for 24 hours. The activation process was carried out in a tubular furnace under a flow of nitrogen (0.1 L/min) at a temperature of 500°C for 2 hours. The sample was further washed with 0.1 M HCl and distilled water until the pH was close to seven. The wet sample was then dried at 105°C for 12 h.

Magnetization process. The magnetization process of AC was carried out using co-precipitation method. First, 0.025 mol of $\text{FeSO}_4 \cdot 7\text{H}_2\text{O}$ and 0.0375 mol $\text{FeCl}_3 \cdot 6\text{H}_2\text{O}$ were each dissolved in 25 ml of distilled water. The two solutions were then mixed, stirred, and heated at 55°C . Afterward, 15 g of AC was added to the solution and stirred continuously for one hour. Followingly, NaOH solution was slowly dropped until pH reached 12. Then, the magnetite-loaded activated carbon was washed with distillation water until the filtrate pH was around seven, separated from solution by a simple magnetic procedure, and dried in an oven at 65°C for 6 hours.

Characterization of Adsorbents. The char, AC, and MAC were analyzed for the surface morphology using a scanning electron microscope (JSM-6360, JEOL, Japan). The specific surface area was calculated by the Brunauer-Emmet-Teller (BET) method from N_2 adsorption/desorption isotherm at 77K using an automated gas sorption apparatus (NOVA 1200, Quantachrome, USA). The Fourier Transform Infra-red (FTIR) spectroscopy (Spectrum 100, PerkinElmer, USA) was used to analyze surface groups of the adsorbents in a range of $400\text{--}4000\text{ cm}^{-1}$. XRD patterns of MAC were recorded by X-ray diffraction type D8 Advanced (Bruker, UK) to investigate crystal structure.

Adsorption Studies. The aqueous Zn^{2+} solution was prepared by diluting $\text{Zn}(\text{NO}_3)_2 \cdot 4\text{H}_2\text{O}$ with distilled water to a certain concentration. Adsorption experiments were performed using 0.3 g of adsorbents and 50 ml of Zn^{2+} solutions with different concentrations which were placed into 100 ml Erlenmeyers. The adsorption was carried out at different initial solution pH with added HCl or NaOH 0.1 N. The Erlenmeyers were shaken for four hours with a speed of 150 rpm to reach equilibrium. The Zn^{2+} concentration in the residual solution was analyzed using atomic absorption spectrometer (AAS) (Perkin Elmer, Model PinAAcle 900F). While, the contact time influence on the Zn^{2+} adsorption onto char, AC, and MAC was investigated by pouring 0.3 g of adsorbent to 50 mL of Zn^{2+} solutions (concentration of 10 mg/L, initial solution pH of 4). The adsorption experiments were carried out at different contact times. The percentage of Zn^{2+} adsorbed was calculated by Eq. 1 [15]:

$$\text{Zn}^{2+} \text{ adsorbed (\%)} = \frac{(C_0 - C_t)}{C_0} \times 100 \quad (1)$$

where C_t is the concentration of Zn^{2+} remaining at time t (mg/L).

Results and Discussion

Characterization of Adsorbents. The SEM micrographs of char, AC, and MAC are shown in Fig. 1. The image of char (Fig. 1a) shows the presence of shallow and constricted pores. In addition, some pores appear to be blocked by tarry substances, resulting from the carbonization process. After the KOH treatment process (Fig. 1(b)), several pores have been enlarged and opened, resulting in the increase of porosity and specific surface area (from $1.2\text{ m}^2/\text{g}$ for char to $325.3\text{ m}^2/\text{g}$ for AC). In this sense, potassium (K) can insert into the char pores and functions as a template to widen the existing pores. When magnetite (Fe_3O_4) was embedded to the AC, the pores partially filled and covered by Fe_3O_4 (Fig. 1(c)), leading to a decrease in specific surface area (from $325.3\text{ m}^2/\text{g}$ for AC to $230.1\text{ m}^2/\text{g}$ for MAC).

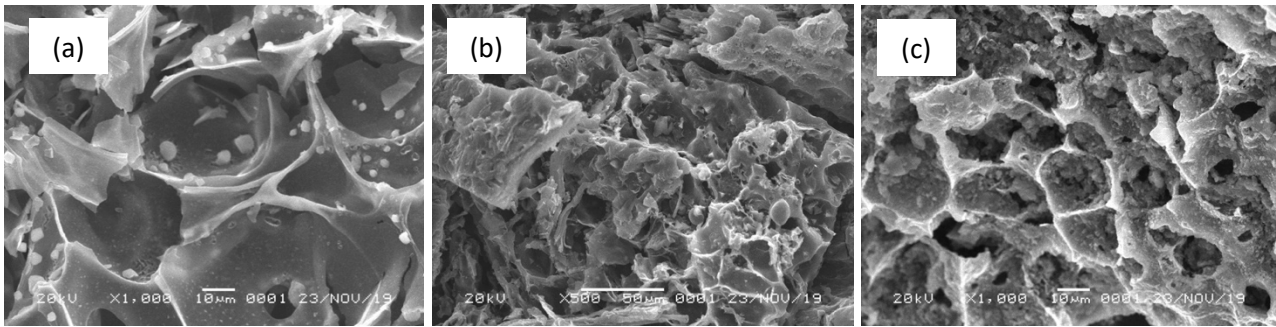


Fig. 1 SEM micrographs of (a) char, (b) activated carbon (AC), and (c) magnetic activated carbon (MAC).

FTIR spectrum analysis was carried out to identify different surface groups on the char, AC, and MAC surface that function as active sites on the Zn^{2+} adsorption. In Fig. 2, all samples have similar spectra, indicating they have similar surface groups. The absorption peak around $3400-3700\text{ cm}^{-1}$ with a maximum at 3406 cm^{-1} represented $-OH$ stretching vibration of hydroxyl groups [8]. The absorption peak at 2925 cm^{-1} was assigned to the $C-H$ group. The peak observed at $1500-1600\text{ cm}^{-1}$ can be attributed to the $C=C$ stretching vibration of aromatic compounds. The band at 1605 cm^{-1} represented $C=O$ stretching vibration, whereas those at 1060.98 cm^{-1} could be assigned to the $C-O$ stretching of the $-OCH_3$ group [8]. After the carbonization and activation process, the position and intensity of some peaks being changed. The band around $3400-3700\text{ cm}^{-1}$ became shallower, which suggested the decrease $-OH$ group while peaks around $500-750\text{ cm}^{-1}$ belong to the Fe_3O_4 (magnetite) [8]. Magnetite was also identified in the XRD pattern of MAC through the presence of peaks at 2θ of 29° , 35° , 43° , 54° , and 63° which correspond to magnetite peak standards (JCPDS No. 96-900-2321).

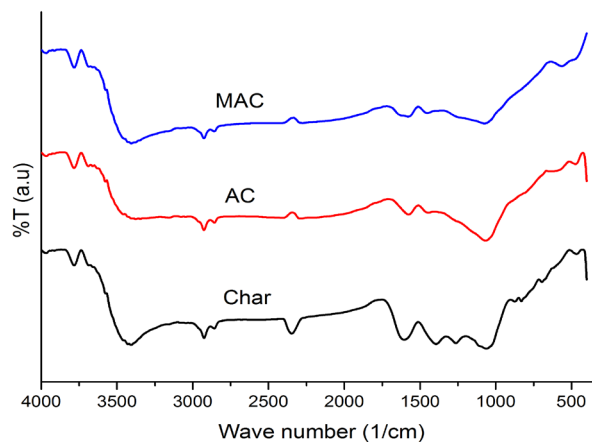


Fig. 2 FTIR spectra of (a) char, (b) activated carbon (AC), and (c) magnetic activated carbon (MAC).

Adsorption of Zinc. The adsorption efficiency of Zn^{2+} onto char, AC, and MAC linearly increased with increases in pH until pH 4 (Fig. 3(a)). In the high acid medium, the phenolic groups on the AC surface will be protonated. Consequently, there is no ionic interaction between the phenolic groups and Zn^{2+} , resulting in the decrease of Zn^{2+} adsorbed. The highest adsorption efficiency was obtained at pH 4 due to the protonation decreased. At a high pH level ($pH > 4$), the decreasing trend was likely caused by the formation of hydroxide complexes of Zn^{2+} , including $ZnOH^+$ and $Zn(OH)_2$. Thus, further experiments in this study were carried out at pH 4. In addition to PH, contact time is an important parameter that provides information on the equilibrium time. As seen from Fig. 3(b), the percentage removal of Zn^{2+} increased rapidly in the first 40 min and after 180 min, most of active sites have been occupied, leading to a linear curve. The effect of initial concentration for Zn^{2+} removal by char, AC, and MAC is shown in Fig. 3(c). It is evident that the higher initial concentration, the lower the percentage removal of Zn^{2+} . However, the amount of Zn^{2+} adsorbed per unit adsorbent mass

increased with increasing initial Zn^{2+} concentration and faster equilibrium was attained at a lower concentration. It may be related to the abundance of vacant sites at lower concentration. In addition, the percentage removal of Zn^{2+} by MAC was higher than that of AC. It may be due to an increase in the number of active sites from magnetite.

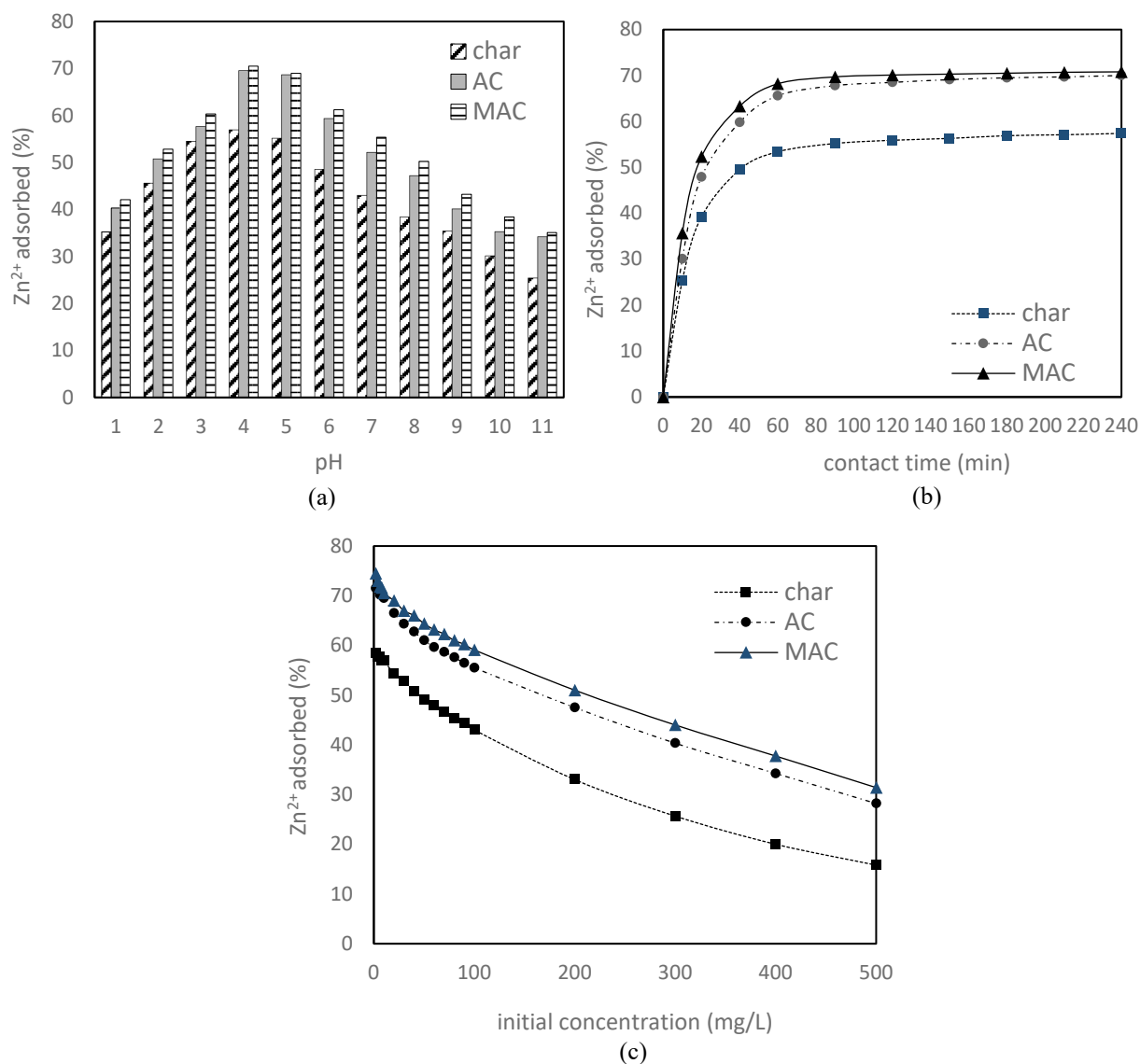


Fig. 3 Effect of (a) pH, (b) contact time, and (c) initial concentration on the removal of Zn^{2+} by char, activated carbon (AC), and magnetic activated carbon (MAC).

Summary

The magnetite (Fe_3O_4) was loaded successfully to the activated carbon (AC) prepared from pineapple crown leaf using KOH as an activator agent. Adsorption experiments showed that magnetic activated carbon (MAC) is an effective adsorbent for zinc removal from aqueous solution. The amount of zinc adsorbed by MAC was higher than AC, although the increase is meaningless.

Acknowledgment

This work was supported by The Directorate for Research and Community Services, Ministry of Research, Technology and Higher Education (Grant Number: 192/SP2H/LT/DRPM/2019).

References

- [1] R. F. Gonzales, M. Calero, Effective removal of zinc from industrial plating wastewater using hydrolyzed olive cake: Scale-up and preparation of zinc-based biochar, *J. Clean. Prod.* 227 (2019) 634-644.
- [2] V. D. A. Cardoso, A. G. de Souza, P. P. Sartoratto, L. M. Nunes, The ionic exchange process of cobalt, nickel and copper (II) in alkaline and acid-layered titanates, *Colloids Surf. A Physicochem. Eng. Asp.* 248(1-3) (2004) 145-149.
- [3] M. Ye, G. Li, P. Yan, J. Ren, L. Zheng, D. Han, S. Sun, S. Huang, Y. Zhong, Removal of metals from lead-zinc mine tailings using bioleaching and followed by sulfide precipitation, *Chemosphere*, 185 (2017) 1189-1196.
- [4] J. E. Efome, D. Rana, T. Matsuura, C. Q. Lan, Effect of operating parameters and coexisting ions on the efficiency of heavy metal ions removal by nano-fibrous metal-organic framework membrane filtration process, *Sci. Total Environ.* 674 (2019) 355-362.
- [5] T. K. Tran, K. F. Chiu, C. Y. Lin, H. J. Leu, Electrochemical treatment of wastewater: Selectivity of the heavy metals removal process, *Int. J. Hydro. Energy*, 42(45) (2017) 27741-27748.
- [6] M. Sillanpaa, M.C, Ncibi, A. Matilainen, M. Vepsalainen, Removal of natural organic matter in drinking water treatment by coagulation: A comprehensive review, *Chemosphere*, 190 (2018) 54-71.
- [7] S. Gogoi, S. Chakraborty, M. D Saikia, Surface modified pineapple crown leaf for adsorption of Cr(VI) and Cr(III) ions from aqueous solution, *J. Environ. Chem. Eng.* 6(2) (2018) 2492-2501.
- [8] W. Astuti, T. Sulistyarningsih, E. Kusumastuti, G. Y. R. S. Thomas, R. Y. Kusnadi, Thermal conversion of pineapple crown leaf waste to magnetized activated carbon for dye removal, *Biores. Technol.* 287((2019) 121426.
- [9] E. Yagmur, Y. Gokce, S. Tekin, N.I. Semerci, Z. Aktas, Characteristics and comparison of activated carbons prepared from oleaster (*Elaeagnus angustifolia* L.) fruit using KOH and ZnCl₂, *Fuel*, 267 (2020) 117232.
- [10] O. Oginni, K. Singh, G. Oporto, B. D. Andoh, L. McDonald, E. Sabolsky, Effect of one-step and two step H₃PO₄ activation on activated carbon characteristic, *Biores. Technol. Rep.* 8 (2019) 100307.
- [11] W. Astuti, R. A. Hermawan, H. Mukti, N. R. Sugiyono, Preparation of activation carbon from mangrove propagule waste by H₃PO₄ activation for Pb²⁺ adsorption, *AIP. Conf. Proc.* 1788(1) (2017) 030082.
- [12] L. Yue, Q. Xia, L. Wang, L. Wang, H. DaCosta, J. Yang, X. Hu, CO₂ adsorption at nitrogen-doped carbons prepared by K₂CO₃ activation of urea-modified coconut shell, *J. Colloid Interf. Sci.* 511 (2018) 259-267.
- [13] K. K. Beltrame, A. L. Cazetta, P. S. de Souza, L. Spessato, T. L. Silva, V. C Almeida, Adsorption of caffeine on mesoporous activated carbon fibers prepared from pineapple plant leaves, *Ecotox. Environ. Safe.* 147 (2018) 64-71.
- [14] S. Y. Gu, C. T. Hsieh, Y. A. Gandomi, Z. F. Yang, L. Li, C. C. Fu, R. S. Juang, Functionalization of activated carbon with magnetic Iron oxide nanoparticles for removal of copper ions from aqueous solution, *J. Mol. Liq.* 277 (2019) 499-505.
- [15] E. Altintig, H. Altundag, M. Tuzen, A. Sari, Effective removal methylene blue from aqueous solutions using magnetic loaded activated carbon as novel adsorbent, *Chem. Eng. Res. Des.* 122 (2017) 151-163.